

NACA RM L50G14a

# NACA

## RESEARCH MEMORANDUM

THE EXTERNAL-SHOCK DRAG OF SUPERSONIC INLETS  
HAVING SUBSONIC ENTRANCE FLOW

By Louis M. Nucci

Langley Aeronautical Laboratory  
Langley Air Force Base, Va.

CLASSIFICATION CANCELLED

Authentic: *NACA R 7 2557* Date: *8/23/54*

By *DATA 9/15/54* See \_\_\_\_\_

CLASSIFIED DOCUMENT

This document contains classified information affecting the National Defense of the United States within the meaning of the Espionage Act, USC 50:31 and 32. Its transmission or the revelation of its contents in any manner to an unauthorized person is prohibited by law.  
Information so classified may be imparted only to persons in the military and naval services of the United States, appropriate civilian officers and employees of the Federal Government who have a legitimate interest therein, and to United States citizens of known loyalty and discretion who of necessity must be informed thereof.

### NATIONAL ADVISORY COMMITTEE FOR AERONAUTICS

WASHINGTON  
December 20, 1950



3 1176 01407 1626

NACA RM L50G114a

UNCLASSIFIED

## NATIONAL ADVISORY COMMITTEE FOR AERONAUTICS

## RESEARCH MEMORANDUM

## THE EXTERNAL-SHOCK DRAG OF SUPERSONIC INLETS

## HAVING SUBSONIC ENTRANCE FLOW

By Louis M. Nucci

## SUMMARY

The external-shock drags of supersonic inlets having circular cross sections have been determined from shadow photographs at a Mach number of 2.70 for a low-external-compression and a high-external-compression inlet.

The calculated mass flows for both types of inlets showed reasonably good agreement with the measured values. The external flow field of the low-external-compression inlet was also measured at one streamwise station and agreed reasonably well with calculated values. As the mass flow of the low-external-compression inlet was reduced, the external-shock drag increased. At 74 percent of the design mass flow, the external-shock drag for this inlet was approximately 6.5 times as great as the drag at design mass flow. For the high-external-compression inlet the external-shock drag at 74 percent of the design mass flow was 11 times as great as the external-shock drag of the low-external-compression inlet operating at the design mass flow.

In cases where the entering mass flow as well as the shock configuration is known it is possible to use a simple approximate method for determining the external shock drag rather than the more laborious procedure involving the use of characteristics. A comparison of the results obtained by the two methods for the present configurations indicated satisfactory agreement.

## INTRODUCTION

The shock-wave drag of bodies of revolution at an angle of attack of  $0^\circ$  in a completely supersonic-flow field can be determined by the method of characteristics (ref. 1). This method has been applied to the determination of the external-shock drag of inlets (refs. 2 and 3).

UNCLASSIFIED

The system, however, cannot be directly applied to the determination of the external-shock drag of inlets operating with subsonic entrance flow or perforations.

In reference 4, a method has been presented which can be used for determining the external-shock drag of supersonic inlets having either supersonic or subsonic entrance flow and/or perforations. The only experimental information needed is a shadow or schlieren photograph of the shock configuration of the inlet and the free-stream Mach number. This method has been applied in the present paper for the determination of the external-shock drag of an inlet having low external compression and different relative mass flows and of an inlet having high external compression at a free-stream Mach number of 2.70.

An approximate method for determining the external-shock drag of bodies having attached or detached frontal shock waves, which was suggested by Dr. A. Ferri of the Langley Aeronautical Laboratory, has also been applied for the determination of the external-shock drag of the inlets investigated. The results obtained by this approximate method have been compared with the results obtained by the more accurate method given in reference 4.

#### SYMBOLS

V	velocity
$\rho$	density
p	pressure
q	dynamic pressure
$c_p$	specific heat at constant pressure
$\gamma$	ratio of specific heats
S	entropy
$\frac{M_E}{M_L}$	relative mass flow, ratio of mass of air that entered the inlet divided by the air which would enter an area equal to the cowl-entrance area in the free stream
D	drag

$D_M$	maximum diameter of inlet
$D_E$	entering-free-stream-tube diameter
$D_L$	entrance diameter of cowling
$D_B$	maximum diameter of central body
$\frac{D_B}{D_L}$	central-body-diameter ratio
$\theta_c$	semicone angle of central body
$\theta_l$	cowling-position parameter, angle between axis of inlet and straight line that connects vertex of cone with lip of cowling
$C_D$	drag coefficient
Subscripts:	
o	refers to stagnation free-stream conditions
l	free-stream conditions
L	local-flow conditions

## DESCRIPTION OF THE INLETS INVESTIGATED

## AND THE TESTING PROCEDURE

The external-shock drag of two types of inlets having subsonic entrance flow was determined in the investigation. The first type of inlet tested had low external compression. The inlet (fig. 1) consisted of a cowling and a central body having circular cross sections. The cowling had an entrance diameter of 1.528 inches with internal-external lip angles of  $0^\circ$ ,  $20^\circ 22'$ . The central body had a  $20^\circ$  semicone-angle tip located at an angle of  $\theta_l = 34^\circ 47'$  with respect to the leading edge of the cowling. The ratio of the maximum diameter of the inlet to the entrance diameter was 1.14. The external-shock drag was determined for the section up to the maximum diameter. In order to obtain different stable mass flows into this inlet, four different maximum central-body diameters were used. For purposes of identification the central bodies are labeled from A to D and are used to identify the inlet-operating condition.

~~CONFIDENTIAL~~

The second type of inlet investigated, designed for a free-stream Mach number of 2.80, had high external compression (fig. 2). The inlet consisted of a perforated cowling and a central body having circular cross sections. It is of interest to investigate the application of the method of reference 4 and the approximate method of the present report to an inlet with perforations, since the method of reference 1 cannot be applied directly to such an inlet. The cowling had an entrance diameter of 1.436 inches and lip angles and perforations as shown. The central body was of the multiple-shock variety and was located at an angle of  $\theta_1 = 24^{\circ}5'$  with respect to the lip of the cowling.

In order to check the calculation procedure (ref. 4), a total-pressure and static pressure rake (figs. 1 and 3) were located on the outside of the low-external-compression-inlet cowling, 1.03 entrance diameters behind the leading edge of the lip. The entering mass flow was measured for both inlets by a calibrated thin-plate orifice.

Tests were made in a tunnel having a test section approximately 3 by 5 inches at a free-stream Mach number of 2.70 using low-humidity air from a large pressurized tank. The model support and the test equipment were similar to those described in reference 3. The Reynolds number of the models tested referred to the inlet-entrance diameter was approximately  $3 \times 10^6$  which corresponds to an inlet having a free-stream-tube diameter of approximately 1.5 feet at an altitude of 60,000 feet.

During each test the entering mass flow was measured and shadow photographs were taken. Pressure recovery was also measured for the high-external-compression inlet. (Values of pressure recovery for the type of inlet having low external compression are available from reference 3.) The inlet mass flow was measured by ducting the air entering the inlet outside the tunnel into a mass-flow meter which consisted of a calibrated thin-plate orifice. The shadowgraph system consisted of a single parabolic mirror mounted 1 focal length from a spark source which introduced parallel light through the test section perpendicular to the axis of the tunnel. In order to minimize any distortion of the head-shock-wave image due to slightly nonparallel light rays, the photographic film was mounted on the glass wall of the tunnel facing the reflected parallel light.

The shadow photographs used for measuring the external-shock drag of the low-external-compression inlet are given in figure 3. The relative mass flow varied from 100 percent for condition A to 74.3 percent for condition D. Condition A corresponds to supersonic entrance flow. Conditions B, C, and D correspond to subsonic entrance flow due to the excessive internal-contraction ratio caused by increasing the maximum diameter of the central body. These latter conditions can be considered as inlets designed for higher Mach numbers. As the relative mass flow is decreased, the frontal shock moves upstream and increases

in intensity. Uneven separation on the cone surface at the lower mass-flow rates causes the detached head shock to vary slightly in intensity axially. Separation on the top surface of the cowling for flow conditions C and D was due to too low a tunnel-pressure ratio. This separation did not affect the shape of the detached shock used (as was established during tests at higher pressure ratios) and, therefore, was disregarded in this analysis.

The shadow photograph used for determining the external-shock drag of the high-external-compression inlet is shown in figure 4. Disturbances due to the air escaping through the perforations can easily be seen to be causing the frontal shock to have an irregular variation. The increase in entropy to the flow behind the frontal shock-wave disturbances caused by the small amount of air escaping through the perforations was assumed to be small and was neglected.

#### DRAG DETERMINATION

##### Characteristics Method

The shock configuration for a supersonic inlet having subsonic entrance flow is shown in figure 5. Because the inlet is operating at a reduced mass flow or Mach number lower than that which permits supersonic entrance flow, a detached frontal shock occurs in front of the inlet. A local separation near the leading edge of the cowling produces a weak secondary shock.

From the shadow photographs shown in figures 3 and 4, the coordinates of the detached frontal-shock wave were determined with a precision comparator. The shadow image of a shock wave consists of a dark and a light line close together. For this analysis the ordinates of the shock wave were read on the upstream side of the dark line. For all the inlets considered, the frontal-shock-wave length used was approximately 1.2 inlet-entrance diameters long.

The general scheme of calculations using the method given in reference 4 is shown in figure 6. From the shape of the frontal-shock wave AF it is possible to construct the characteristics net ABCD and, therefore, the flow field around the inlet. From continuity considerations, this system also provides the location of the point E in the free stream. The location of the point E establishes the internal mass flow. Knowing the flow properties along the surface AD and the free-stream conditions, the momentum equation can be applied to the fluid passing both AE and AD, and the drag force acting on the stream tube ED can be determined. In this analysis the external-shock drag has been defined as the resultant of the absolute-pressure forces acting on the stream tube which wets the surface of the cowling.

## Approximate Method

The method of measuring the external-shock drag of inlets having subsonic entrance flow given in reference 4 requires the calculation of many points of the flow field with the characteristics system and, therefore, some simplifications have been considered in order to obtain approximate values in a shorter time.

As for the characteristic method, the only experimental information needed for the approximate method is a shadow or schlieren photograph of the shock configuration, the free-stream Mach number, and, for inlets, the entering-free-stream-tube radius. The general scheme for the engineering method is shown in figure 7. The detached shock wave AC is given and the entering-free-stream-tube radius is known from mass-flow measurements. The maximum diameter of the cowling at the point D is known; therefore, assuming a cylindrical body following the cowling, which does not change the pressure drag, the point D' at infinity, where the pressure is again atmospheric, is also known. Knowing the mass flow passing through AC and the intensity of the shock AC, it is possible to determine the change of each elemental stream tube due to the increase in entropy. Therefore, the area of BD' at infinity or the value of  $y_B$ , where the pressure is again atmospheric, can be determined with the following equation:

$$y_B^2 = 2 \int_{y_C}^{y_A} \frac{\rho_1 v_1}{\rho_1' v_1'} y \, dy + y_{D'}^2$$

where, from reference 5,

$$\frac{\rho_1}{\rho_1'} = e^{\frac{\Delta S}{c_p}}$$

and

$$\frac{v_1}{v_1'} = \frac{1}{\sqrt{1 - \frac{2 \left( e^{\frac{\Delta S}{c_p}} - 1 \right)}{(\gamma - 1) M_1^2}}}$$

From the entropy variation along AC, the momentum along BD' can be calculated, and from momentum considerations the forces along CD' and AB can be determined. In order to determine the force acting on

the stream tube CD', which is equivalent to CD, or the external-shock drag it is necessary to know the force acting on the stream tube AB; however, only the flow quantities at the points A and B and the frontal area of the stream tube AB are known, the pressure variation along the stream tube AB is not known. Reference 6 shows that if a shock-wave length of approximately 10 body radii is used for determining the shock drag of bodies of revolution, the pressure variation acting on the stream tube AB is small and can be neglected. In many practical applications, however, the available shock-wave length is small because of the large model size relative to the tunnel, and the force acting on the stream tube AB cannot be neglected; therefore, some approximation for estimating the force acting on the stream tube AB was made. In order to evaluate this force, two alternative assumptions were made in this analysis as to the pressure variation on the frontal area of the stream tube AB. From these assumptions, the force along AB was obtained so that an approximate value of the external-shock drag could be determined. By assuming that the pressure changes linearly with the radius on the frontal area of the stream tube AB from the value at A to the free-stream value at B, a lower limit of the external-shock drag can be obtained; whereas assuming that the pressure on the frontal area of the stream tube AB is constant and equal to the pressure at A, an upper limit of the external-shock drag will generally be obtained. The difference between the two values decreases as the point A moves away from the body.

## RESULTS AND DISCUSSION

### Characteristics Method

Applying the method given in reference 4 to the four shadow photographs of the low-external-compression inlet shown in figure 3, the flow field behind the shock, the entering-free-stream-tube radius, and the external-shock drag were determined. The shock wave on the same side of the photograph as the external pressure tubes was used for the calculations so that the measured Mach number distributions could be compared with the calculated Mach number distributions.

A typical characteristics net calculated for flow condition B is shown in figure 8. The corresponding calculated stream lines are shown in figure 9. The characteristic nets for flow conditions C and D follow the same general trend as flow condition B, so they are not shown. For the design condition A, the method given in reference 1 could have been used to determine the flow properties of the inlet since the flow around the inlet was completely supersonic. However, in order to check the precision of the method given in reference 4, this latter method was used for determining the external-shock drag.

Figure 10 shows the calculated pressure distributions on the cowling surface as a function of the relative distance from the leading edge of the cowling for the four mass-flow conditions considered. For condition A, which corresponds to completely supersonic external flow, the pressure distribution follows a trend generally expected when the pressure tends to the conical value at infinity. The pressure rise due to the finite cowling-lip deviation for the condition of completely supersonic external flow is shown on the vertical axis. If the mass flow is reduced, a detached shock occurs in front of the inlet. The sharp lip causes a local separation on the cowling surface with a subsequent weak shock. Curves B, C, and D correspond to the pressure distributions calculated for the reduced mass-flow conditions. Because the calculations cannot be extended to the lip by the method of reference 4, only part of the local separation phenomenon is indicated by the pressure-distribution curves. The calculations show that, as the mass flow is reduced, the cowling pressure decreases.

The measured Mach number distribution at one station 1.03 inlet diameters behind the leading edge of the cowling for inlet-flow conditions B and C is compared with the calculated values in figure 11. In general, the agreement is relatively good.

Using the method given in reference 4, a point was determined in the free stream which corresponded to the stream tube which wetted the surface of the cowling. This point determines the entering-free-stream-tube radius. The mass flow corresponding to this radius was then compared with the measured entering-mass-flow values. This comparison, in terms of the relative free-stream-tube diameter  $\frac{D_E}{D_L}$  is plotted as a function of the central-body-diameter ratio  $\frac{D_B}{D_L}$  in figure 12. The solid line corresponds to the calculated values and the circle symbols corresponds to the measured values. As the central-body-diameter ratio is increased, the relative mass flow is decreased. The calculated and measured values show very good agreement.

The external-shock drag coefficients determined with the method given in reference 4 are shown in figure 13 as a function of the measured relative mass flow. The external-shock drag coefficients are referred to both the calculated entering-free-stream-tube area and the inlet-entrance area. As the relative mass flow is reduced, the external-shock drag coefficient rises. Referred to the entering-free-stream-tube area, the external-shock drag coefficient for the inlet operating at the design condition is 0.0997, whereas approximately a 26-percent decrease in mass flow corresponds to an external-shock drag coefficient of 0.641.

In order to get a better idea of the large increase in external-shock drag as the mass flow is reduced, the drag in pounds has been calculated using the drag coefficients presented in figure 13 for a free-stream-tube diameter of 1.5 feet at an altitude of 60,000 feet. The drag in pounds for the inlet operating at the design mass flow is 135 pounds, whereas for the inlet having a relative mass flow of 0.74 the drag is 870 pounds.

The second type of inlet investigated had high external compression (fig. 2). The inlet consisted of a multiple-shock central body and a high lip-angle cowling with 158 perforations around the leading edge of the cowling. The large number of perforations around the cowling lip permits the flow phenomenon to be considered as an axial-symmetrical phenomenon. For inlets having perforations, the flow field about the inlet cannot be determined directly with the characteristics method (ref. 1), even though the flow is supersonic at the lip of the cowling, because an unknown quantity of air escaping through perforations alters the flow field. A shadow photograph of the shock configuration for this inlet was shown in figure 4. The maximum pressure recovery measured for this inlet was 0.76. The measured relative mass flow for this inlet was 0.75, whereas the value obtained with the method given in reference 4 was 0.74. The external-shock drag coefficient for this inlet referred to the entering-free-stream-tube diameter is 1.11. The high external-shock drag for this type of inlet is not due solely to the air escaping through the perforations. Tests were made for the same inlet configuration with and without cowling perforations. The relative mass flow for the same configuration without perforations was 0.762. A comparison between the shock configurations of the high-external-compression inlet with and without perforations showed that the frontal shock waves were practically of the same intensity; therefore, the high external-shock drag for inlets having high external compression is due primarily to the large lip angles required for this type of inlet. The drag in pounds for this inlet, assuming a free-stream-tube diameter of 1.5 feet at an altitude of 60,000 feet, is 1,520 pounds. The inlet having high external compression has high pressure recovery compared with the values obtained in reference 3 for the low-drag inlets. However, the high lip angles required for this type of inlet give high external-shock drag which usually overbalances the increase in thrust due to the higher pressure recovery.

#### Approximate Method

Figure 14 gives the low-external-compression-inlet external-shock drag coefficient results obtained with the approximate method as a function of the measured relative mass flow. The external-shock drag coefficients are referred to the entering-free-stream-tube area. As

the relative mass flow increases or the intensity of the frontal shock decreases, the precision of values obtained by the approximate method increases. A comparison of the values obtained with the approximate method and the results obtained with the characteristics method shows good agreement.

#### CONCLUSIONS

From an analysis of the results of an investigation of the two supersonic inlets having subsonic entrance flow, the following conclusions are indicated:

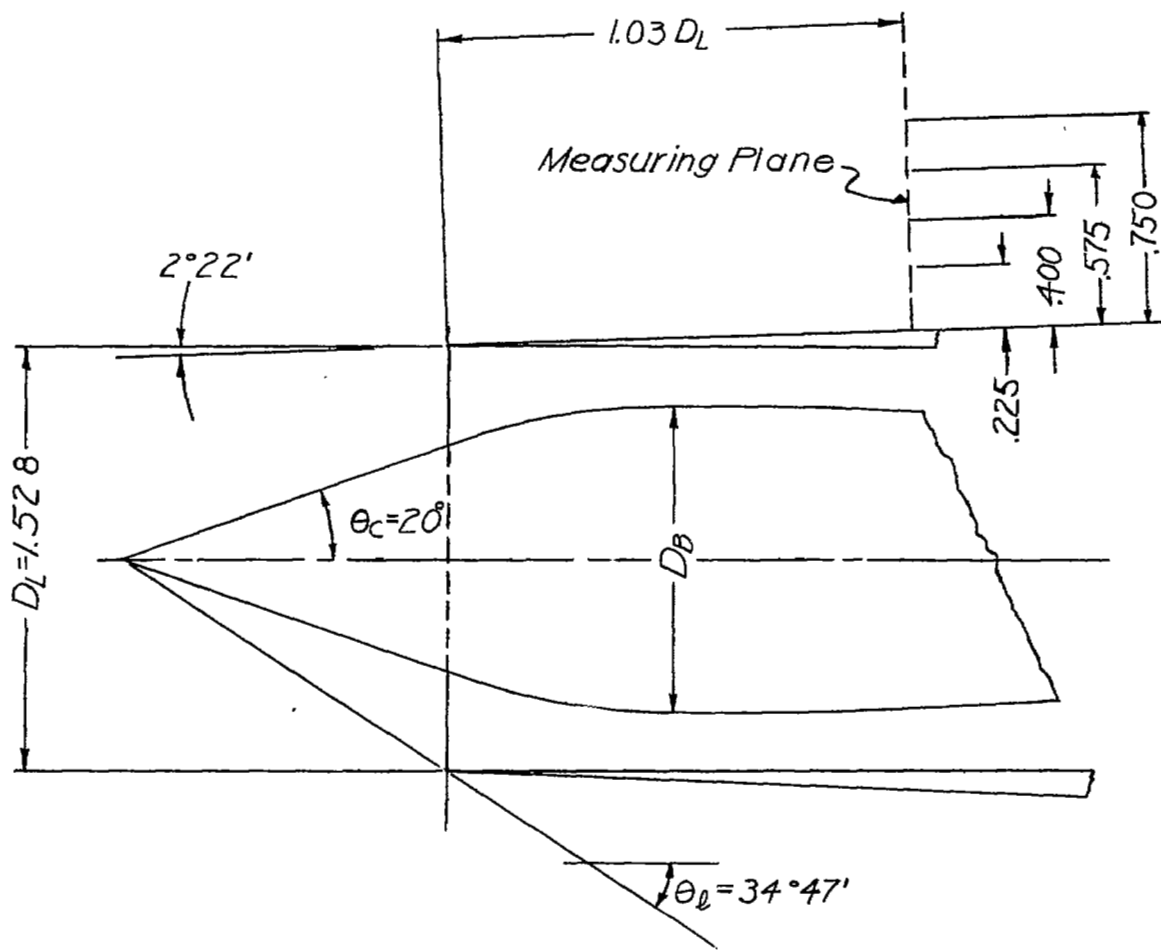
1. The external-shock drag of an inlet having low external compression increased greatly as the relative mass flow was reduced. At 74 percent of the design mass flow, the external-shock drag for this inlet was approximately 6.5 times as great as the external-shock drag at the design mass flow.
2. The external-shock drag of the inlet having high external compression was much larger than for an inlet having low external compression at a Mach number of 2.70. At 74 percent of the design mass flow, the external-shock drag for the inlet having high external compression was 11 times as great as the external-shock drag of the low-external-compression inlet operating at the design mass flow.
3. A comparison between measured and calculated entering-mass-flows and external-flow fields indicates that the method given in NACA TN 1808 adequately determines the flow properties of an inlet having subsonic entrance flow.
4. A simple approximate method which is less laborious than the procedure involving the use of characteristics can be used with satisfactory accuracy if both the shock configuration and entering mass flow are known.

Langley Aeronautical Laboratory  
National Advisory Committee for Aeronautics  
Langley Air Force Base, Va.

~~CONFIDENTIAL~~

## REFERENCES

1. Ferri, Antonio: Application of the Method of Characteristics to Supersonic Rotational Flow. NACA Rep. 841, 1946.
2. Ferri, Antonio, and Nucci, Louis M.: Preliminary Investigation of a New Type of Supersonic Inlet. NACA RM L6J31, 1946.
3. Ferri, Antonio, and Nucci, Louis M.: Theoretical and Experimental Analysis of Low Drag Supersonic Inlets Having a Circular Cross-Section and a Central Body at Mach Numbers of 3.30, 2.75, and 2.45. NACA RM L8H13, 1948.
4. Ferri, Antonio: Method for Evaluating from Shadow or Schlieren Photographs the Pressure Drag in Two-Dimensional or Axially Symmetrical Flow Phenomena with Detached Shock. NACA TN 1808, 1949.
5. Ferri, Antonio: Elements of Aerodynamics of Supersonic Flows. The MacMillan Co., 1949, pp. 58-61.
6. Munk, M. M., and Crown, J. Conrad: The Head Shock Wave. Naval Ordnance Lab. Memo. 9773, Aug. 25, 1948.

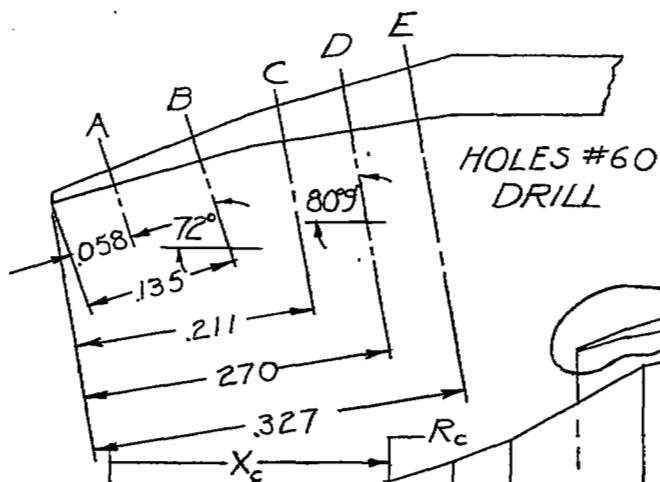


FLOW CONDITION	$D_B/D_L$
A	.654
B	.688
C	.720
D	.757

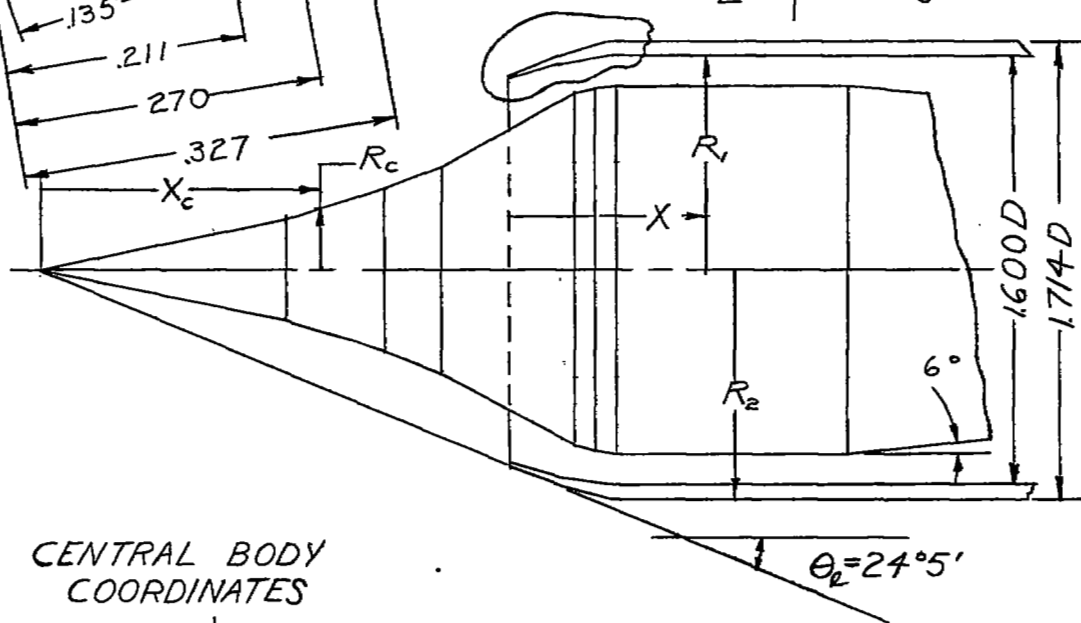
NACA

Figure 1.- Low-external-compression inlet.

ENLARGED VIEW COWLING LIP



ROW	NO OF HOLES
A	44
B	61
C	25
D	25
E	3



CENTRAL BODY COORDINATES

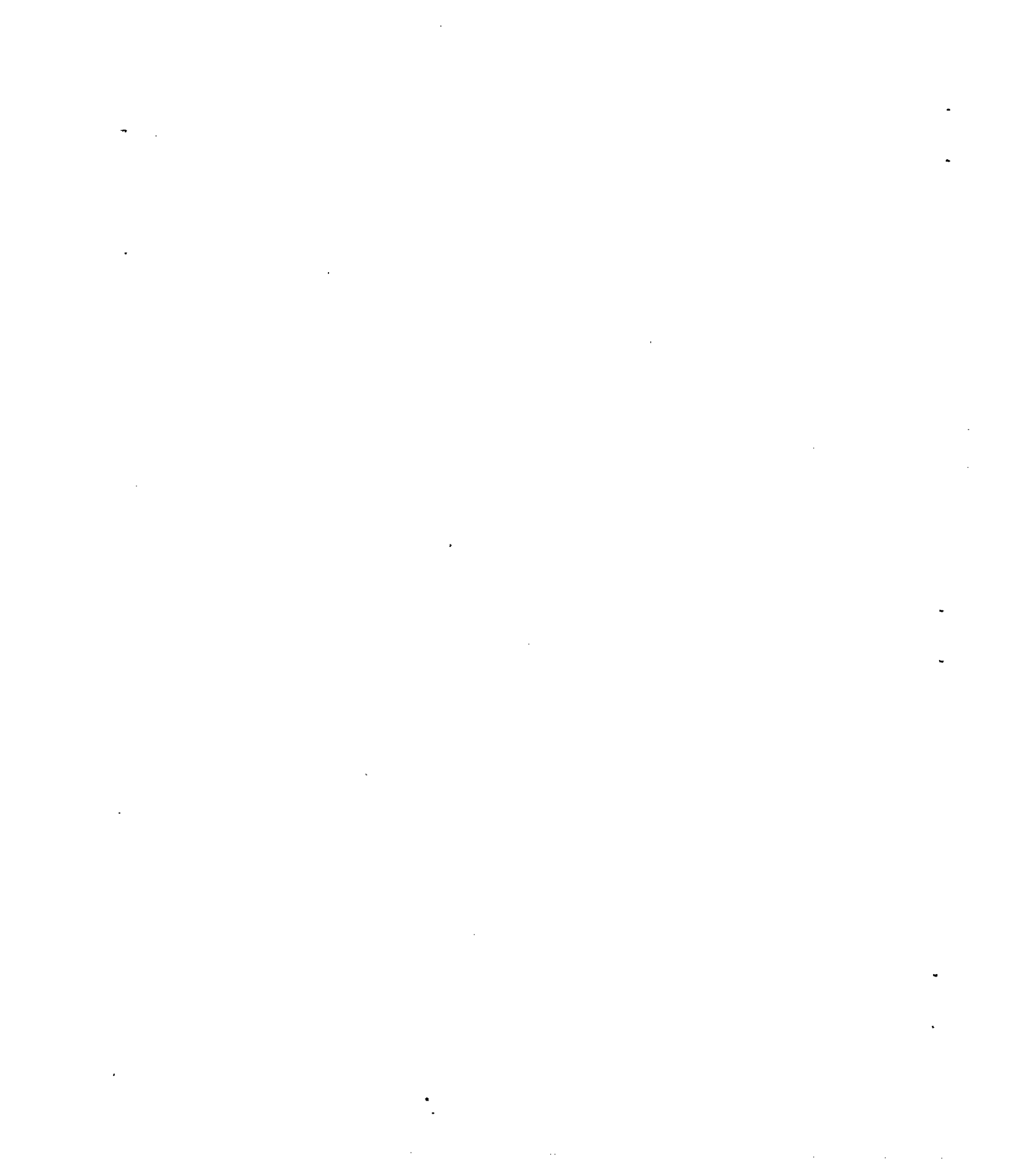
$X_c$	$R_c$
0	0
.857	.189
1.192	.302
1.384	.385
1.845	.658
1.916	.678
1.989	.687
2.790	.687

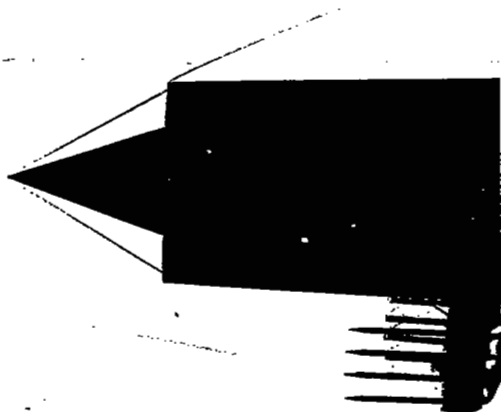
COWLING COORDINATES

X	$R_1$	$R_2$
0	.718	.724
.171	.770	.800
.347	.800	.857



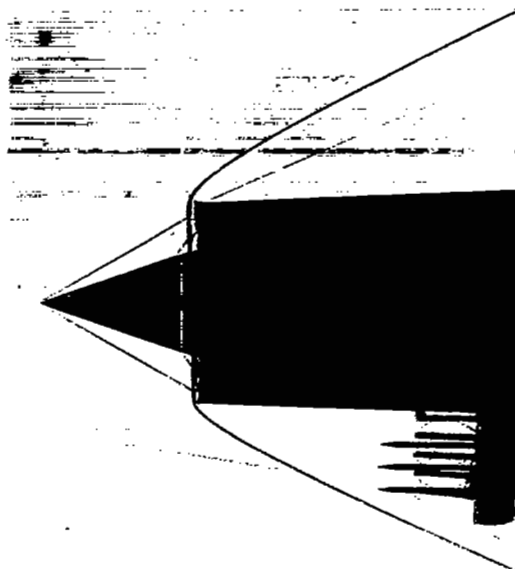
Figure 2.- High-external-compression inlet.





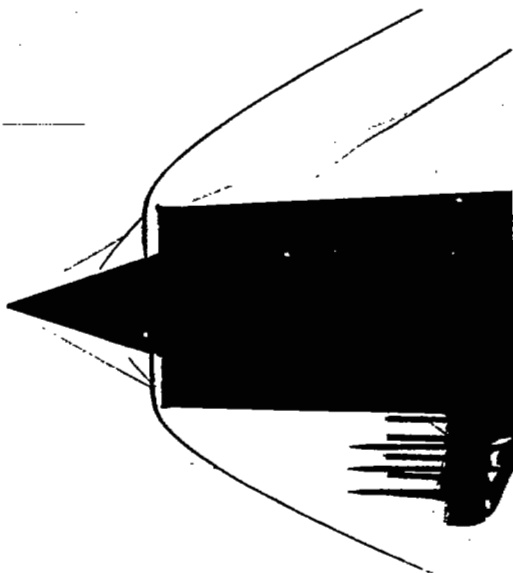
Flow condition A

$$\frac{M_E}{M_L} = 1.00$$



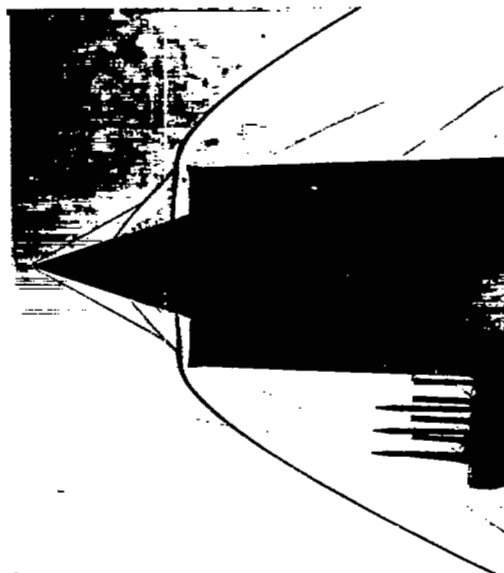
Flow condition B

$$\frac{M_E}{M_L} = 0.928$$



Flow condition C

$$\frac{M_E}{M_L} = 0.830$$



Flow condition D

$$\frac{M_E}{M_L} = 0.743$$

Figure 3.- Shadow photograph of low-external-compression inlet at a Mach number of 2.70.

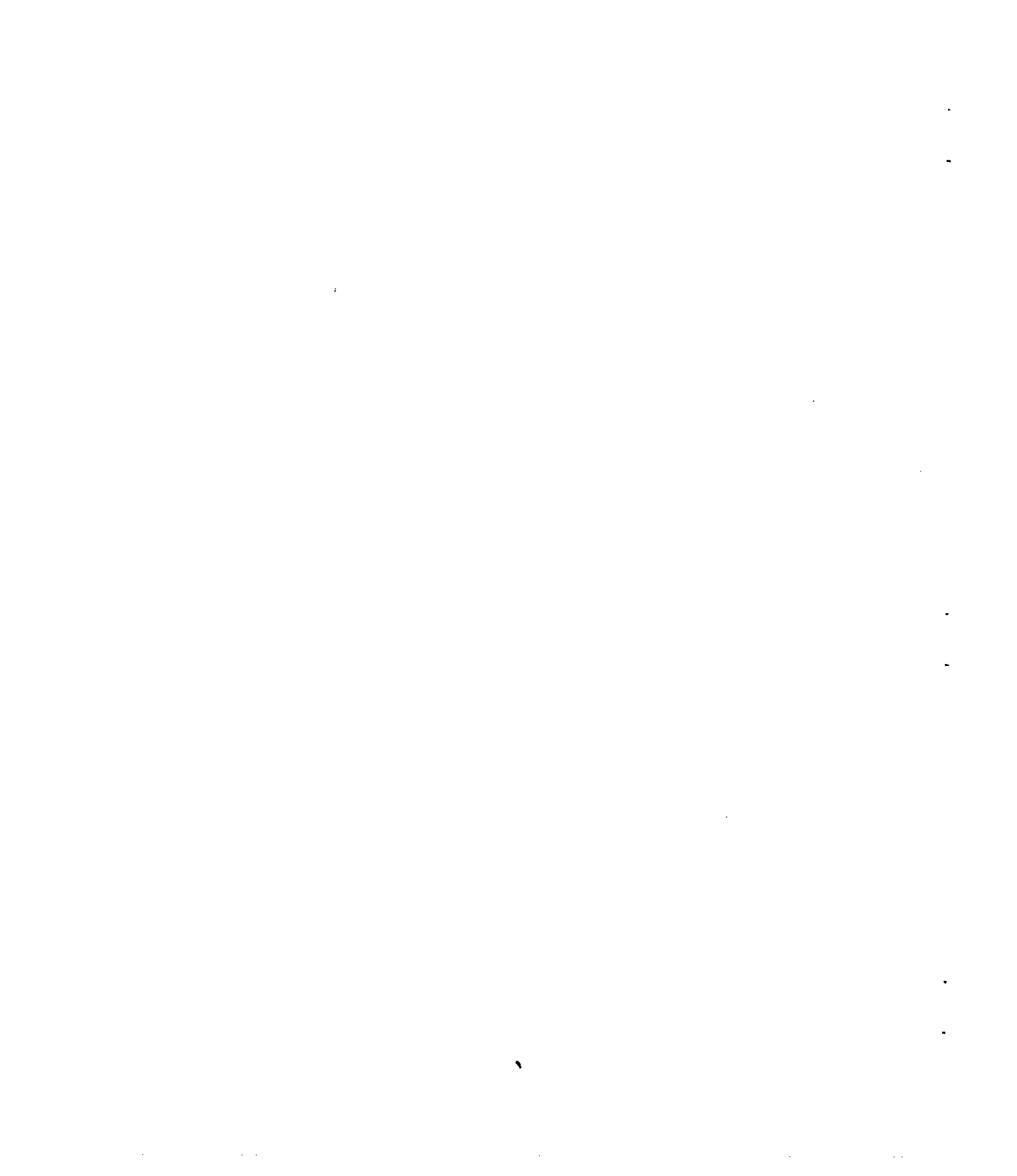
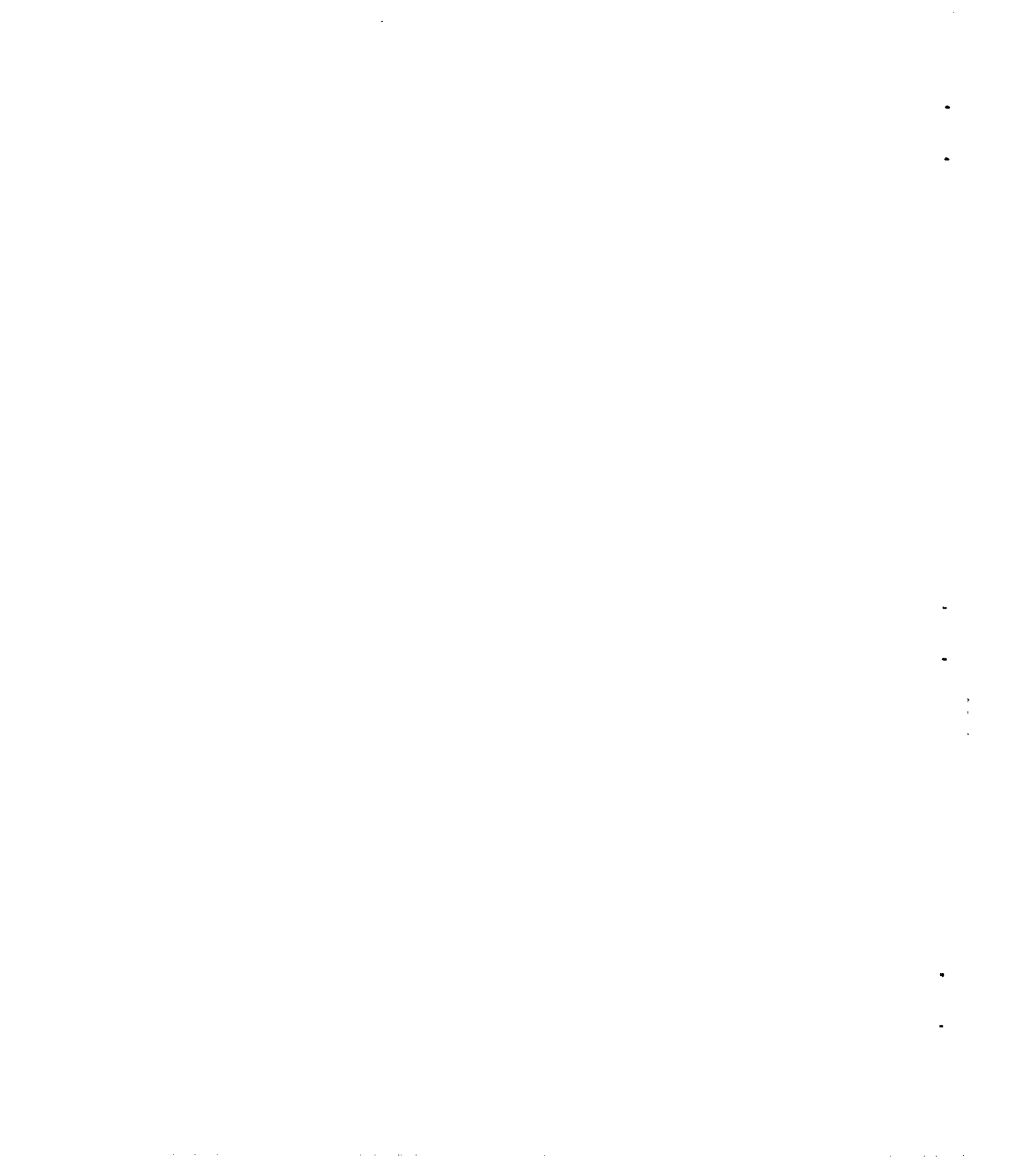




Figure 4.- Shadow photograph of high-external-compression inlet at a Mach number of 2.70.



L-64916



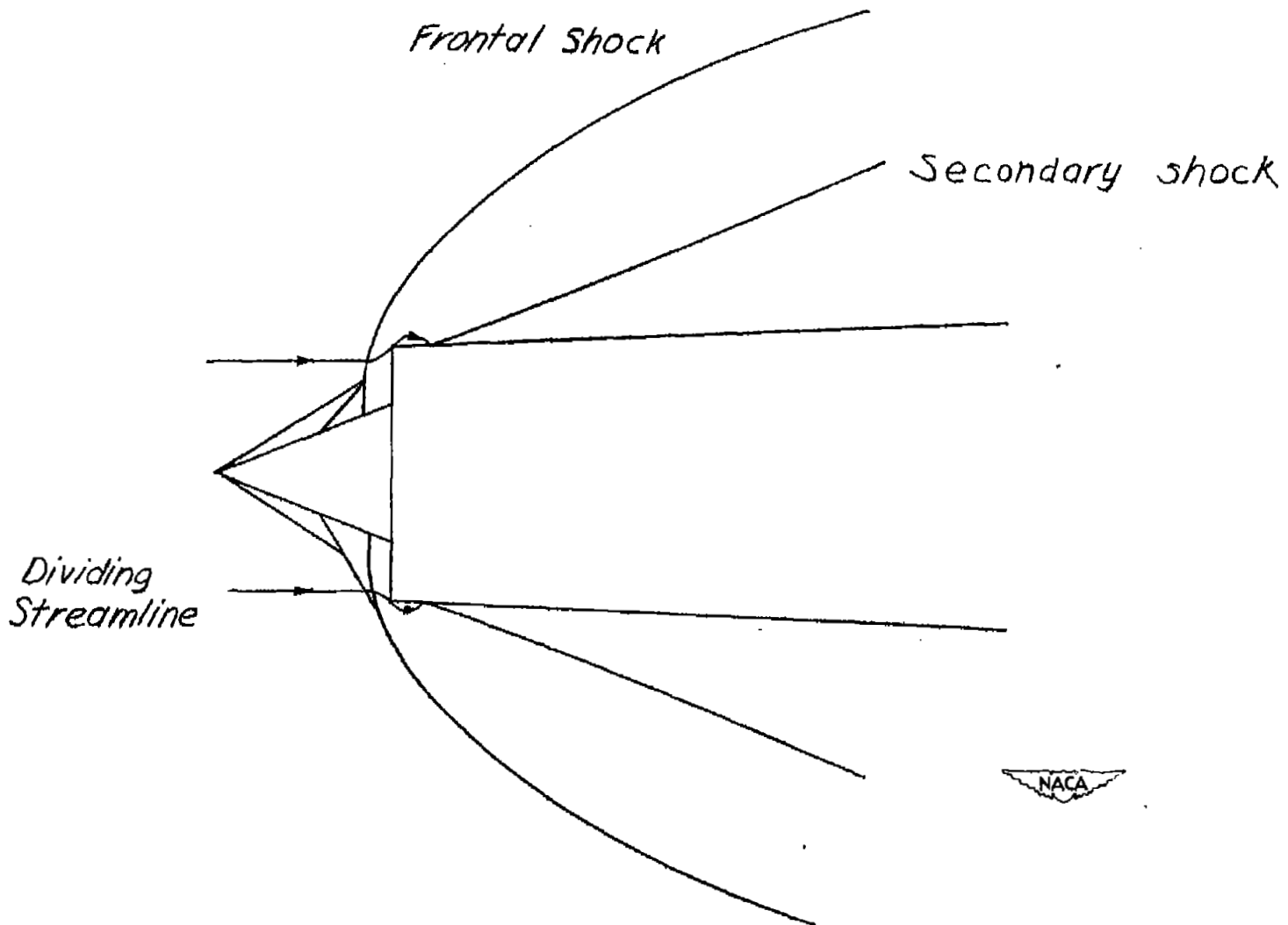


Figure 5.- General shock configuration for inlet having subsonic entrance flow.

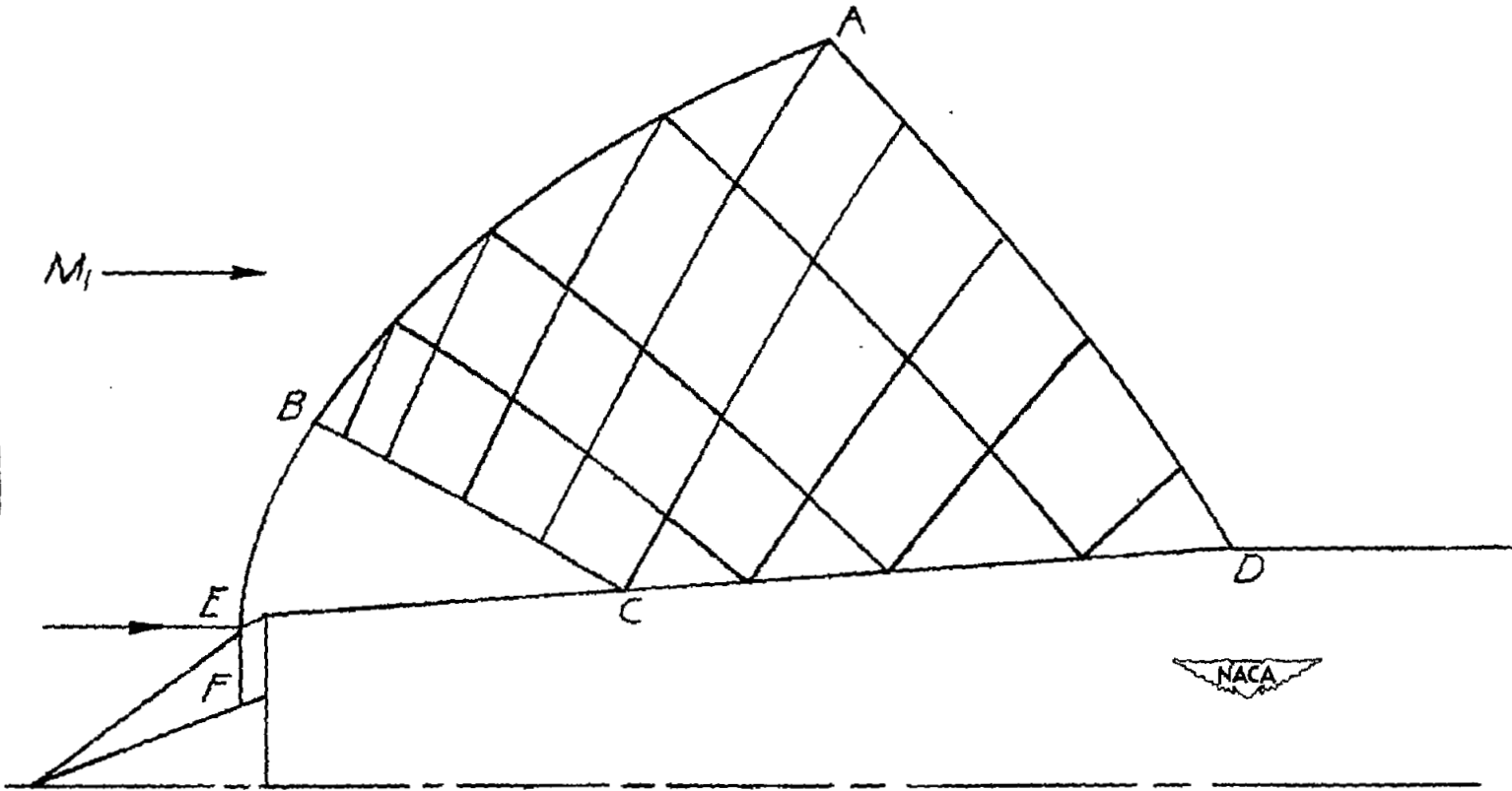


Figure 6.- General scheme used for characteristics calculations.

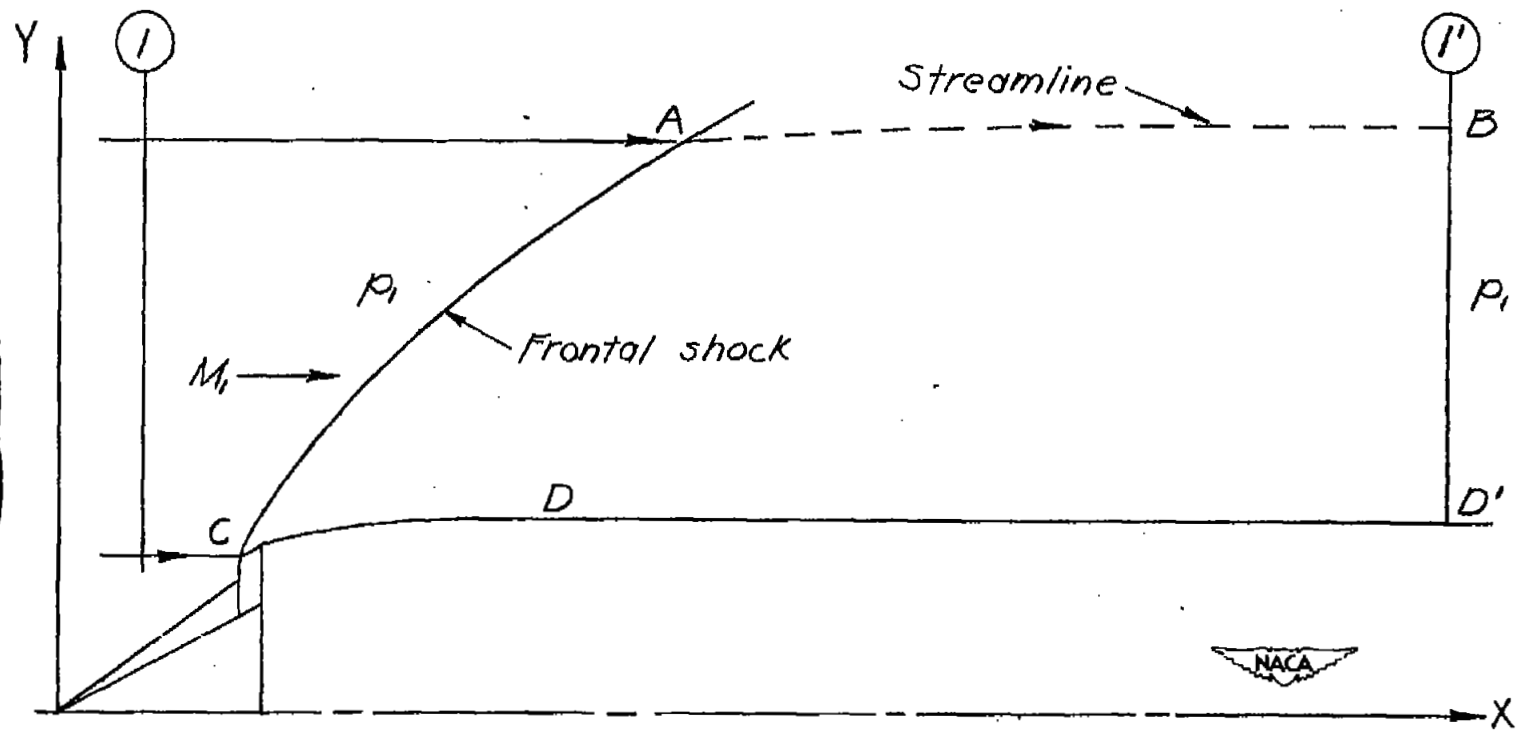


Figure 7.- General scheme for determining the external-shock drag with the engineering method.

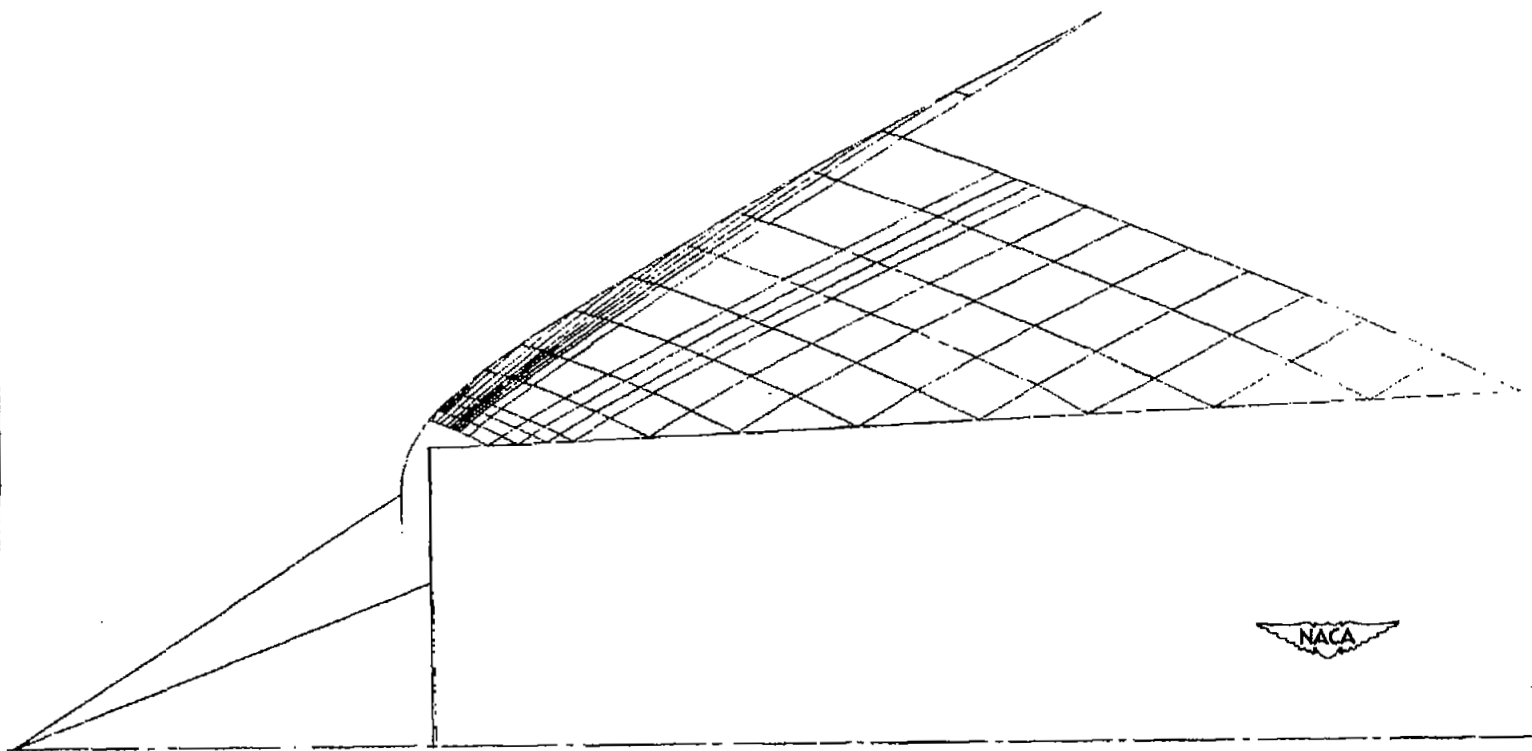


Figure 8.- Characteristics net calculated from shadow picture for low-external-compression inlet for flow condition B,  $M = 2.70$ .

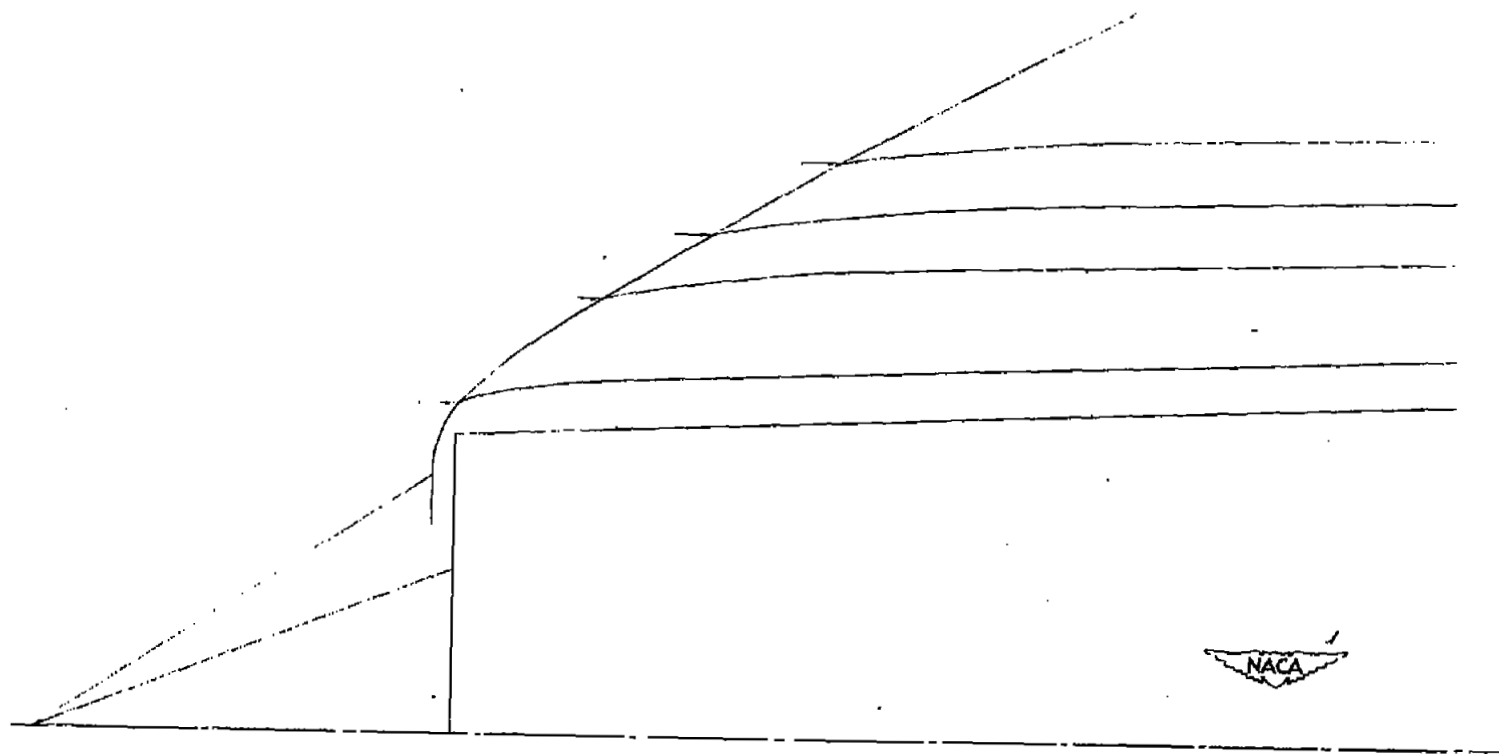


Figure 9.- Streamlines calculated from shadow picture for low-external-compression inlet for flow condition B,  $M = 2.70$ .

Calculated pressure  
distribution on cowl surface,  $P_L/P_1$

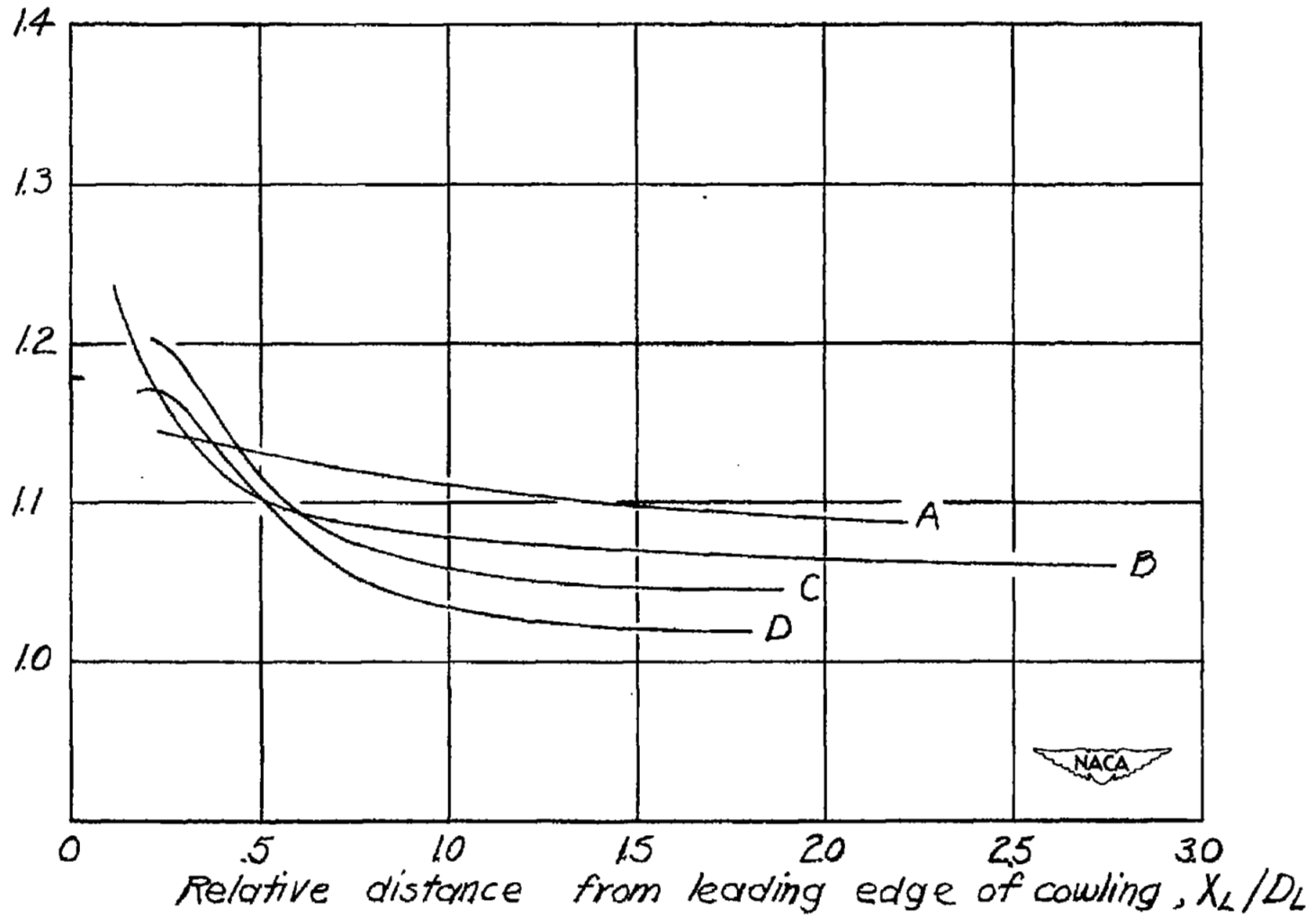


Figure 10.- Pressure distribution on surface of low-external-compression inlet cowl calculated from shadow photographs.

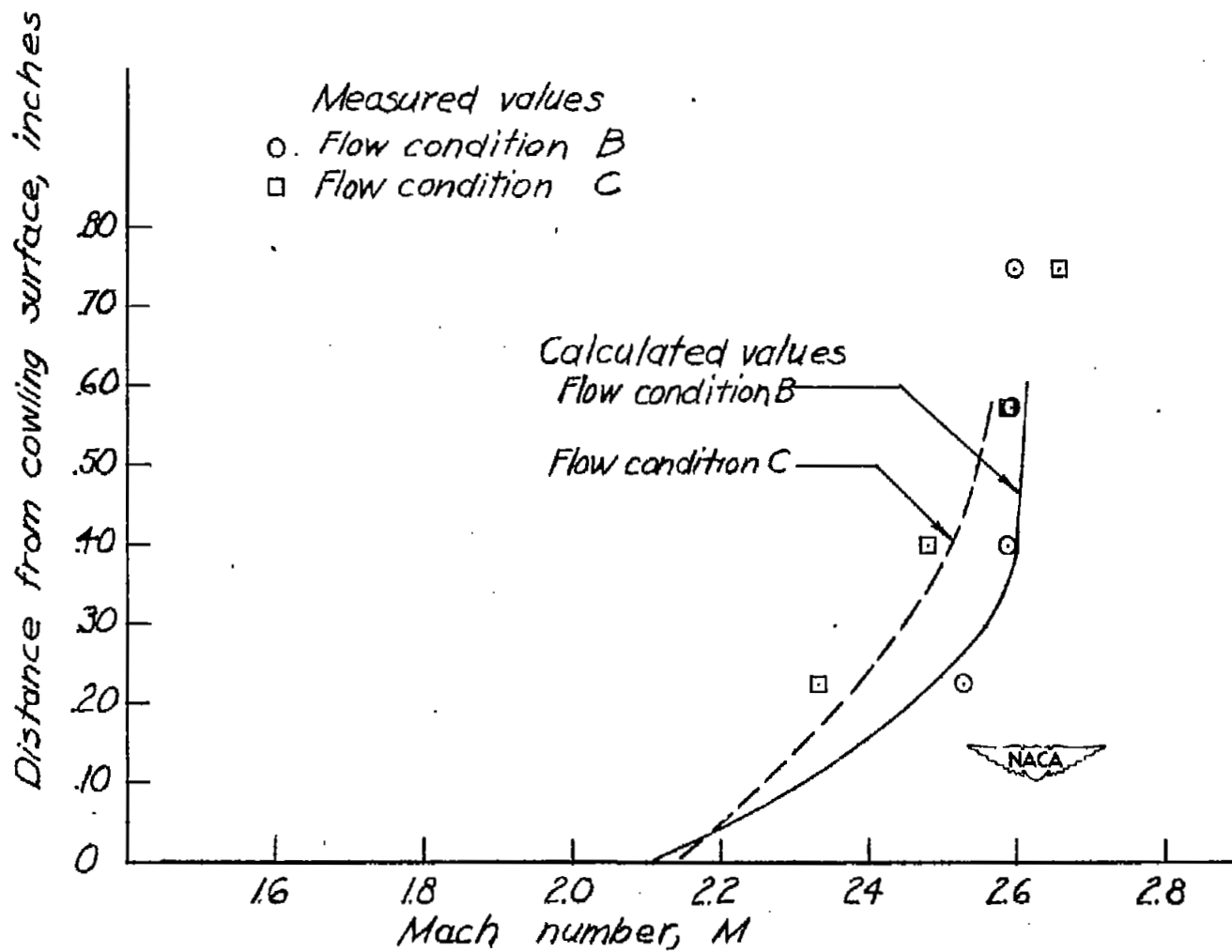


Figure 11.- Mach number distribution 1.03 inlet diameters behind leading edge of the low-external-compression inlet cowling for flow conditions B and C.

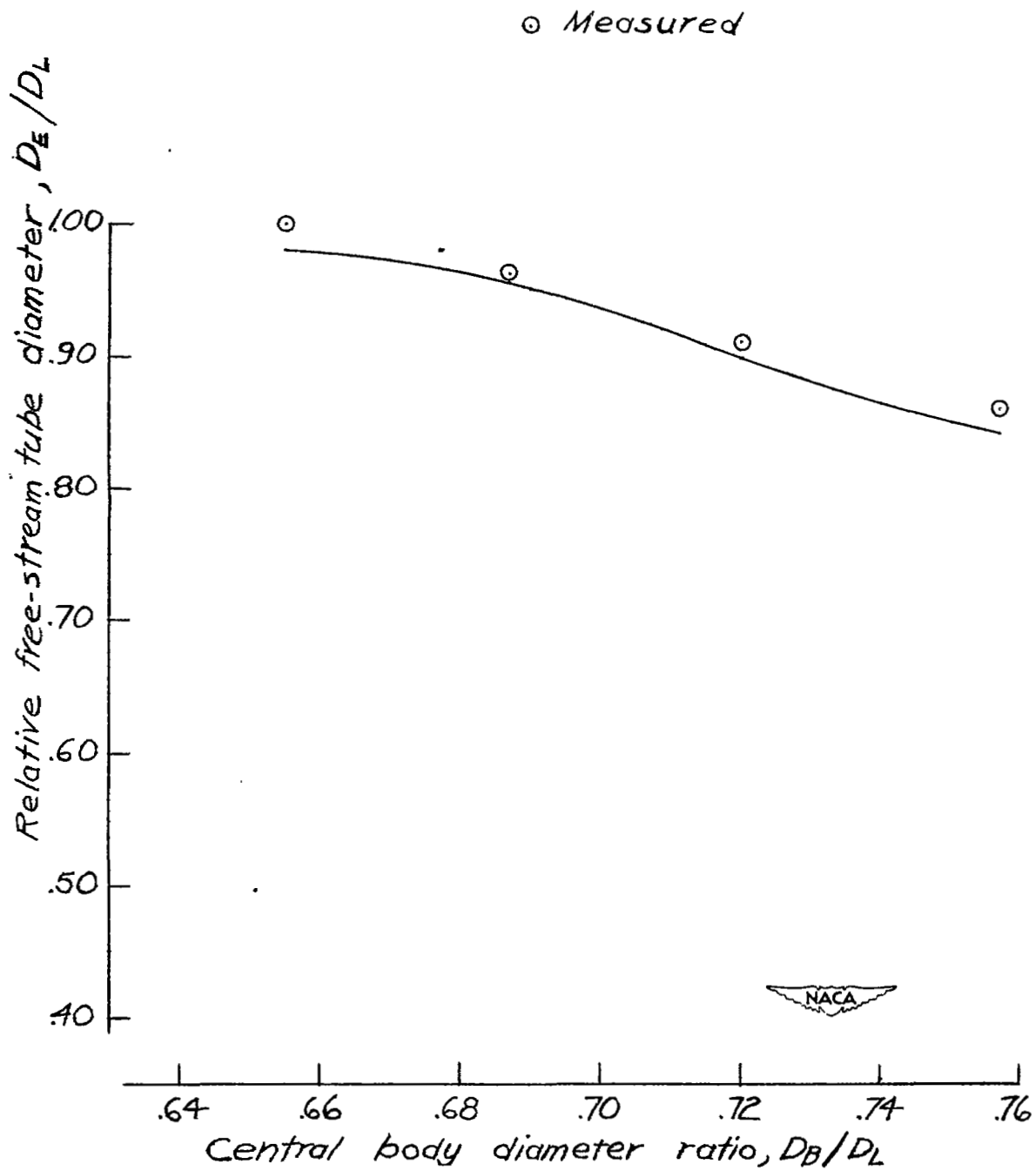


Figure 12.- Relative free-stream-tube diameter as a function of the central-body diameter ratio for the low-external-compression inlet.

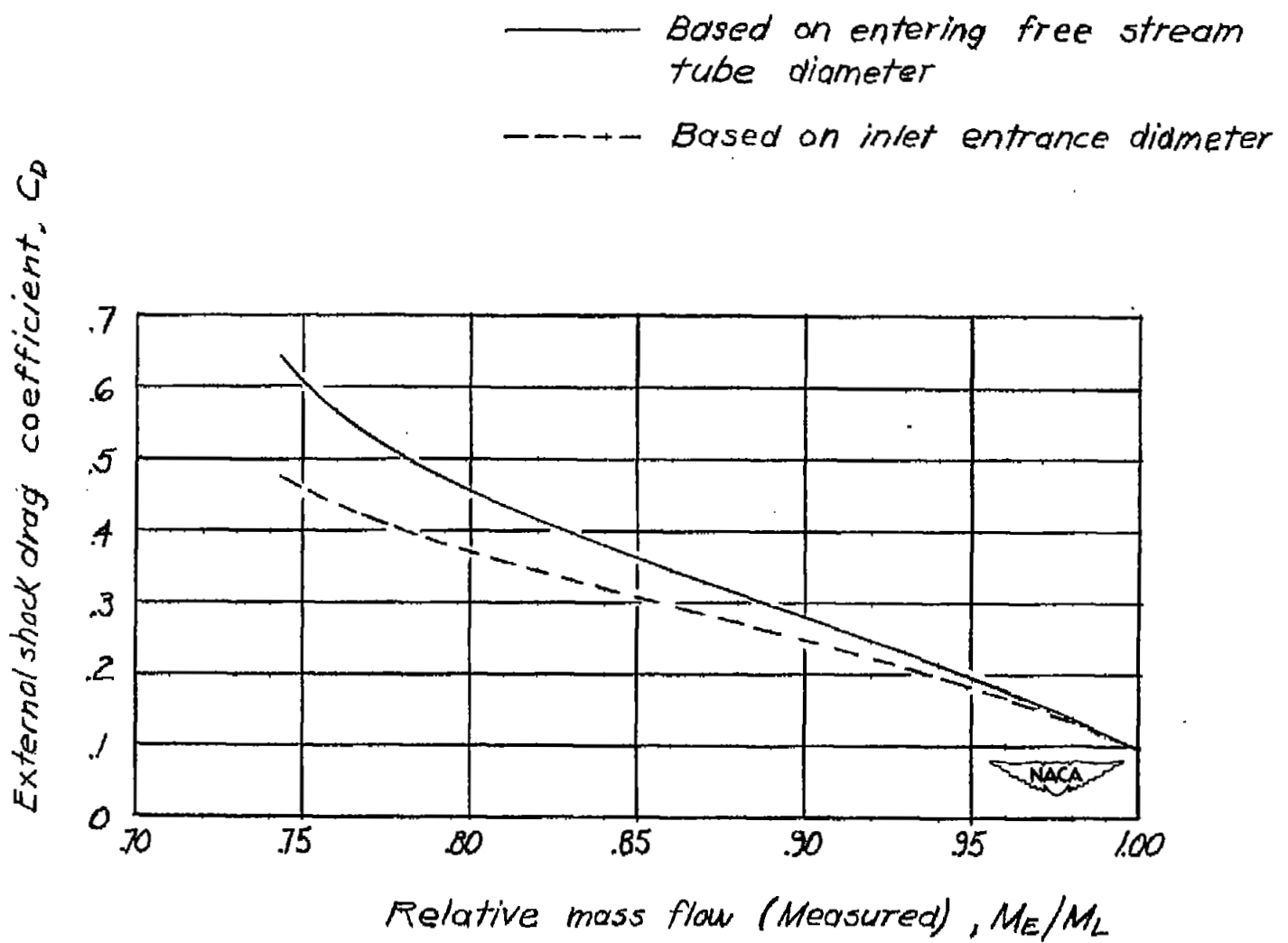


Figure 13.- External-shock drag coefficient as a function of the relative mass flow for the low-external-compression inlet.

External-shock drag coefficient,  $C_D$

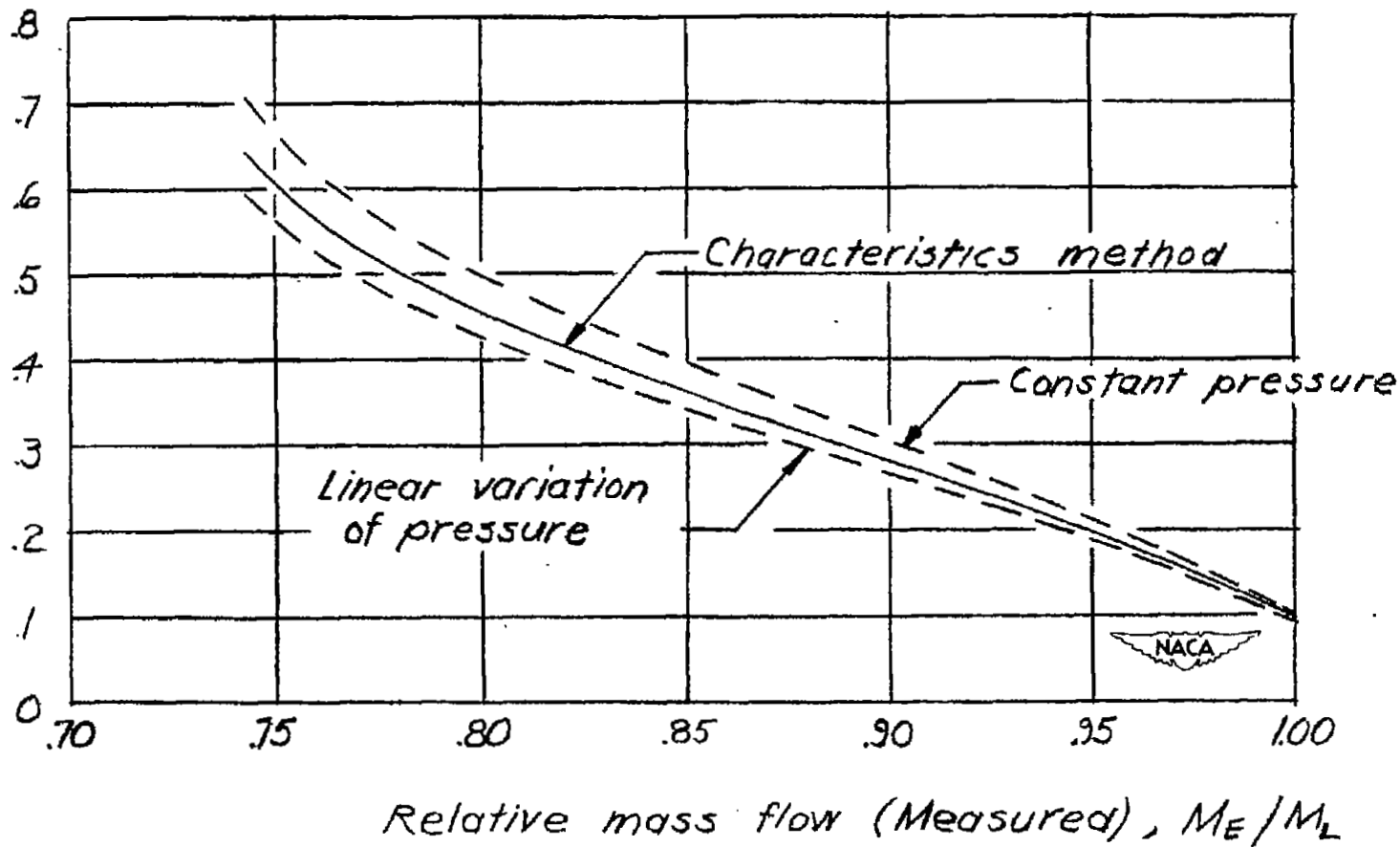


Figure 14.- External-shock drag coefficient as a function of the relative mass flow for the low-external-compression inlet, as determined by various methods.